Available online at www.sciencedirect.com
ScienceDirect
Journal of Power Sources 165 (2007) 49–57
JOURNAL OF POWER SOURCES
www.elsevier.com/locate/jpowsour

Metal foams as flow field and gas diffusion layer in direct methanol fuel cells

Srikanth Arisetty, Ajay K. Prasad, Suresh G. Advani *

Fuel Cell Research Laboratory, Department of Mechanical Engineering, University of Delaware, Newark, DE 19716, USA

Received 27 October 2006; received in revised form 3 December 2006; accepted 5 December 2006
Available online 15 December 2006

Abstract

Metal foams are routinely used in structures to enhance stiffness and reduce weight over a range of platforms. In direct methanol fuel cells, the controlled porosity and high electrical conductivity of metal foams provide additional benefits. Performance studies were conducted with direct methanol fuel cells incorporating metal foams as the flow field. The influence of the foam pore size and density on cell performance was investigated. The performance of similar density metal foams but with different pore sizes was non-monotonic due to the opposing trends of electrical contact and CO_2 removal with pore size. In contrast, for metal foams with the same in-plane pore size, the performance improved with increasing density. Because the cell operates in a diffusion-dominated regime, its performance showed a strong dependence on methanol concentration and a moderate dependence on methanol flow rate. The feasibility of using metal foams as a gas diffusion layer (GDL) was also explored.

Keywords: Direct methanol fuel cells; Metal foam; Gas diffusion layer; Bipolar plates; Multifunctional; Composites

1. Introduction

Direct Methanol fuel cells are a promising power source for a range of portable and low power applications. Many power systems such as those used by the military require optimization in power generation, energy storage and material usage. Examples include energy conversion devices for soldier-portable sensing equipment and communication devices, next-generation ground vehicles utilizing hybrid power trains, or unmanned aerial vehicles or robotic applications whose current range and performance is severely curtailed by battery life [1,2]. As many of these systems incorporate structural and/or armor materials, important system-level weight/volume savings can be realized by employing multifunctional materials that simultaneously offer both power generation or energy storage capabilities along with structural enhancement [2]. Such multifunctional composites can combine multiple functions in a single component. For example, the core in a composite sandwich structure can also serve as components of a direct methanol fuel cell (DMFC) and provide auxiliary power.

Core materials such as open cellular metal foams possess good structural and conductive properties and can therefore replace bipolar plates in fuel cells. The bipolar plate physically separates individual fuel cells in a stack while electrically connecting them, and directs fuel and oxidant gas streams to individual cells [3,9–11]. Traditionally, they are machined from graphite and designed for maximum performance and power density. Several types of channel configurations have been used for the gas flow field in bipolar plates [3–6]. These include parallel, serpentine, multiple serpentine, interdigitated, and fractional flow fields. However, graphite being brittle yields a system design that is not optimized for structural strength. For structural performance and weight savings, graphite plates can be replaced with open cellular metal foams [2]. In this design, a traditional MEA is sandwiched between two metal foam flow fields and covered with a composite skin, resulting in a strong lightweight structural element that can also produce auxiliary power (Fig. 1). Moreover, foams with a wide range of structural properties and permeabilities can be fabricated with ease to meet the multifunctional requirements of the chosen application.

Apart from structural properties, compared to traditional flow fields, metal foams offer advantages in enhancing two-phase flow and current-collecting capacity. For example, efficient removal of carbon dioxide at high current densities is an impor-

* Corresponding author. Tel.: +1 302 831 8975; fax: +1 302 831 3619.
E-mail address: advani@udel.edu (S.G. Advani).

0378-7753/$ – see front matter © 2006 Elsevier B.V. All rights reserved.
doi:10.1016/j.jpowsour.2006.12.008

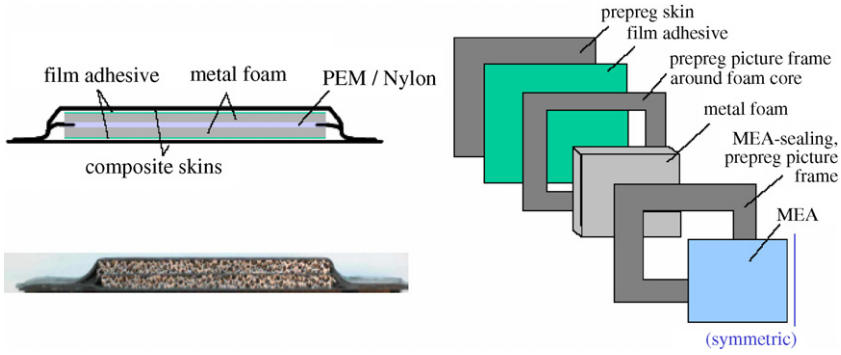

Fig. 1. Cross-section of a multifunctional structural composite fuel cell (with permission from [2]).

tant factor that influences the performance of DMFCs. Three anode flow field functions can influence the cell performance: (i) the anode flow field supplies methanol to the membrane electrode assembly. To enhance performance, the methanol transport to the catalyst layer should be maximized while limiting crossover to the cathode through the membrane; (ii) the anode flow field should efficiently remove carbon dioxide. An accumulation of CO_2 bubbles near the MEA can reduce the cell performance [5,7]; (iii) the anode flow field collects current from the gas diffusion layer (GDL). Effective current collection from the GDL would also enhance performance.

Arico et al. [4] compared the performances obtained using serpentine and interdigitated channels as flow fields in DMFCs. Scott et al. [5] studied the performance characteristics with various steel meshes as flow beds. Other groups have conducted preliminary investigations using porous flow fields for the reactant H_2 in proton exchange membrane fuel cell (PEMFC) [3,8]. The current study uses metal foams, as the porous flow field for DMFCs. Methanol must flow through the GDL as it travels towards the catalyst layer from the flow field. Therefore, the GDL also plays a major role in determining the mass transfer characteristics. Literature suggests that carbon cloth has better gas management characteristics than carbon paper [12,13]. Metal foams are porous and conducting, and hence could potentially also perform the functions typically required of the GDL, thus introducing the possibility of eliminating the GDL from the fuel cell assembly. Accordingly, metal foam consisting of two distinct layers possessing different pore sizes (larger pores constituting the flow field, and smaller pores replacing the GDL) can be placed in direct contact with the catalyst-coated membrane. Pore size can be tailored to improve the cell performance. Oedeggard et al. [12] have performed various studies in DMFCs by changing the GDL type and hence the pore structure.

It should be noted that metal foams should be selected to withstand the strong corrosive environment prevalent within the fuel cell. Electrons released during the reaction travel through the metal foam due to the potential difference developed. Consequently, there exists the possibility of an electrochemical reaction between the methanol solution and the metal foam. While Cu, Al and Ni are common materials selected for metal foams, sensitivity to such reaction is the lowest with Ni.

In the present work, we have examined the performance of a DMFC in which metal foams with different pore size and density serve as the flow field. We also report on studies using two-layer metal foam with different pore sizes that serve the functions of the flow field and the GDL, respectively. Finally, we examine the metal foams after a period of use in the DMFC with a scanning electron microscope (SEM) for indications of corrosion.

2. Experimental details

2.1. DMFC components and assembly

The cell employed in our experiments was designed and fabricated in our laboratory (Fig. 2). A commercially available MEA with carbon cloth GDL on either side was sandwiched between two square plates of metal foams that serve as the flow field, as well as the current collectors. Carbon cloth GDL enhances the transport of the two-phase flow (CO_2 bubbles and methanol), and it cushions the contact between the catalyst layer and the metal foam. The anode catalyst loading was 4 mg cm^{-2} carbon-supported 1:1 Pt–Ru, with 2 mg cm^{-2} carbon-supported Pt on the cathode side. The polymer electrolyte membrane was Nafion

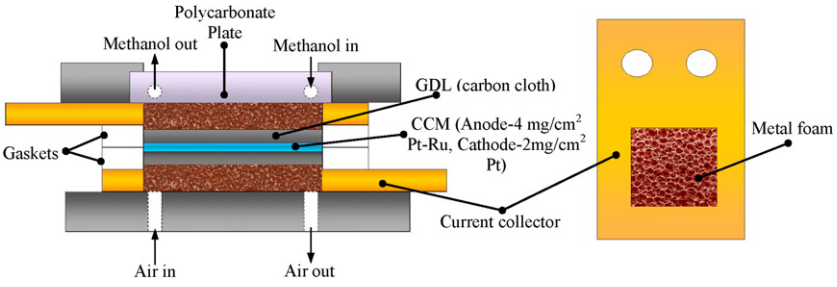

Fig. 2. Transparent operational DMFC incorporating metal foams as flow field.

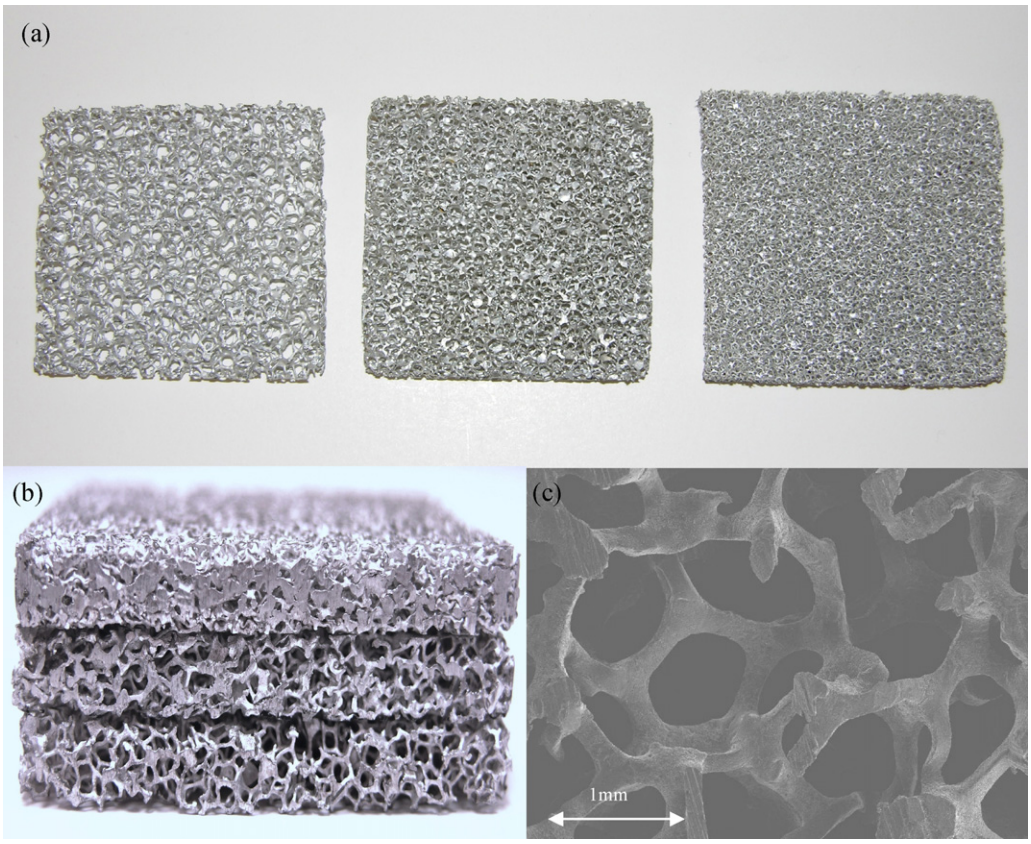

Fig. 3. Metal foams: (a) 10, 20 and 40 ppi (left to right) with 6–8% density. (b) Cross sectional view of 6–8, 12–16 and 18–24% density (bottom to top) with 20 ppi. (c) SEM image of 20 ppi metal foam.

117, and the active area of the MEA was 25 cm^2. As shown in Fig. 2, the methanol enters the metal foam from a spanwise trench inlet cut into the foam at its upstream end; methanol is supplied to this trench from a manifold containing five equi-spaced holes. The methanol then travels away from the trench along the in-plane direction of the foam and exits through a similar spanwise trench at the downstream end. Aluminum plates of 4.72 mm thickness were machined to friction fit the metal foam of dimensions 50.8 mm × 50.8 mm × 6.35 mm. These aluminum plates were designed to support the metal foams and serve as current collectors. The cell temperature was controlled using two electrical heating plates (250 W) positioned against the cell retaining end plates.

One challenging aspect of the design was to prevent damage to the membrane from the rough metal foam surface. Accordingly, 3.17 mm thick gaskets were placed between the MEA and the aluminum plate to absorb the stresses during tightening of the screws while assembling the cell. An important design feature of our cell is that the anode side is made transparent to allow for direct visualization of the two-phase flow dynamics.

2.2. Flow field design and GDL

Two sets of experiments were conducted. In one set, the aluminum metal foam was used as the flow field with conventional GDLs. In the second set, in addition to aluminum metal foam serving as the flow field, the GDL was replaced by either a stainless steel mesh, or nickel metal foam with smaller pores.

For the first set of experiments, cell performance was recorded for five different aluminum foams used as the flow field representing different densities and pore sizes (Fig. 3). Three of them had pores per linear inch (ppi) of 10, 20 and 40, with a density of 6–8%. The remaining two foams had a ppi of 20, with densities of 12–16 and 18–24%, respectively. The ppi characterizes the pore size of the foam. Foam density is defined as the weight fraction of the foam with respect to a solid aluminum block occupying the same volume as the foam. Foams with 12–16 and 18–24% density are fabricated by compressing the 6–8% density foams by a factor of two and three, respectively, along the thickness direction. Typically, metal foams with 6–8% density are isotropic in nature, whereas higher density foams are anisotropic. The pore size in the in-plane direction for foams with different densities does not change for the same ppi.

Traditionally, carbon cloth and carbon paper are used as GDLs in fuel cells. The second set of experiments explored the use of alternate GDL materials such as a stainless steel metal mesh, and Ni metal foam of very high ppi, and compared their performance with traditional carbon cloth GDL. Hence, this set consisted of tests with the following three GDLs: (i) stainless steel mesh (316 stainless steel, 72 ppi, 0.094 mm wire diameter) (ii) Ni foam (2 mm thick with 94 ppi, and 95% porosity); and (iii) Avcarb^{TM} 1071HCB carbon cloth (17.3–21.3 warp cm^{-1}, 16.5–20.5 fill cm^{-1}). In all the three cases, 40 ppi, 6–8% density

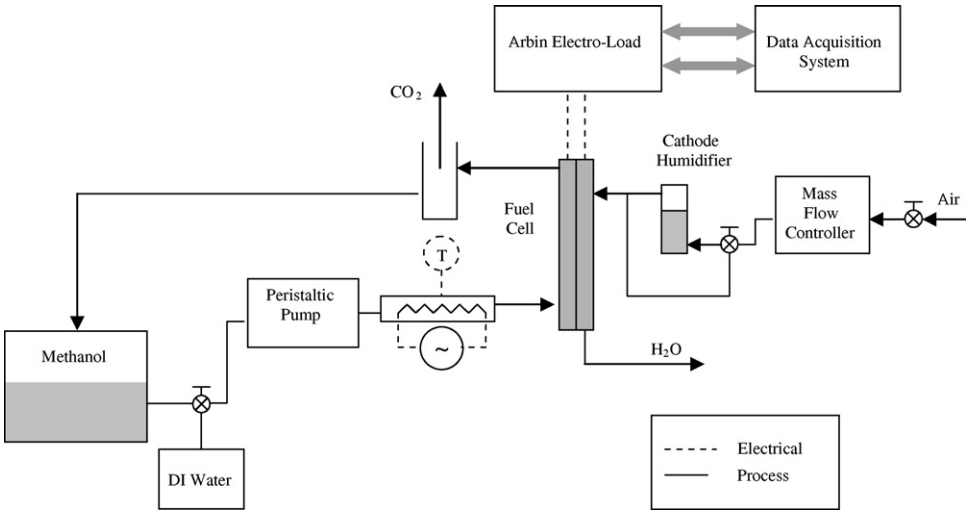

Fig. 4. Schematic diagram of the DMFC loop.

metal foam was used as the flow field. The MEAs employed in this set of experiments were prepared by assembling these GDLs over the catalyst-coated membrane.

2.3. Operating conditions

The schematic of the testing loop is shown in Fig. 4. Methanol solution (2 M) from a supply tank is heated in-line to 50 °C and injected into the DMFC by a peristaltic pump. Unreacted methanol and product CO_2 exit from the fuel cell to a settling chamber, which allows the CO_2 to escape to the atmosphere. The methanol is returned to the supply tank where it is recycled for further reaction. A 5 l batch of methanol solution is used so that the methanol concentration is not significantly altered during the experiment. Furthermore, all experiments are performed under the same cathode operating conditions: a constant airflow rate of 400 standard cubic centimeter per minute (SCCM) and back-pressure of one bar. The operating temperature of the fuel cell is maintained at 50 °C. Before and after every test, the cell is conditioned by flushing with DI water for 15 min. DI water ensures that any methanol in the membrane is removed by diffusion. Cell voltage versus current density is measured by incrementally increasing the current from open circuit and measuring the cell potential at steady state.

3. Results and discussion

3.1. Polarization behavior and power output with metal foam as flow fields

Although a maximum performance of 52 mW cm^{-2} was achieved at 60 °C, the operating temperature for all the tests reported here was lowered to 50 °C to minimize methanol evaporation. Methanol evaporation was further controlled by employing only 6.8% by weight methanol in our experiments. Initial baseline tests were conducted with a serpentine channel, and it was confirmed that our DMFC's performance compared well with results reported in the literature.

Fig. 5 compares the performance of three different aluminum metal foam based fuel cells (different ppi but of constant density of 6–8%) against a conventional 10 cm^2 serpentine channel. The maximum power density obtained using the serpentine channel is comparable with that of metal foams. The serpentine channel shows a lower OCV of 0.45 V, but produces higher current densities. Based on our calculations, the metal foam provides an approximate methanol flow velocity of 0.03 cm s^{-1} whereas the single serpentine channel provides a flow velocity of 7 cm s^{-1} at a volume flow rate of 4 ml min^{-1}. Higher velocities in the serpentine channel would contribute to an increased convective flux to the catalyst layer leading to both an increased crossover at low current densities resulting in a lower OCV, as well as better mass transport at high current densities. Furthermore, at higher current densities, CO_2 bubbles impeding the mass transport will be flushed out more effectively due to higher velocities.

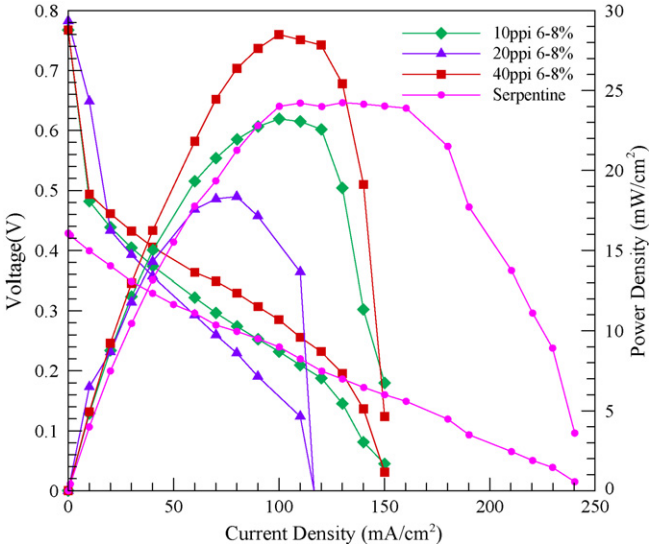

Fig. 5. Comparison of polarization and power density data for DMFC with three different metal foams (varying ppi but constant density).

The cell using 40 ppi gave the best performance. A monotonic trend in performance with ppi was not observed. The variation in the architecture of the foam produces different mass transfer and conductive characteristics. A larger pore size promotes detachment of CO_2 bubbles from the GDL, allowing for more efficient removal of CO_2, and therefore more efficient transport of reactant to the catalyst sites. Hence, mass transfer characteristics improve as the pore size increases (i.e. decreasing order of ppi from 40 and 20 to 10 ppi). On the other hand, a larger pore size implies that electrons must travel larger in-plane distances overcoming larger electrical resistances along the cloth surface before they can be collected by the nearest rib of the metal foam, resulting in less effective current collection. This is significant because the in-plane resistance of the carbon cloth can exceed the through-plane resistance [5].

The above hypothesis can be supported as follows: the in-plane and through-plane resistances are given by

$$R_I \approx \frac{\rho_I L}{Wt}, \qquad R_T \approx \frac{\rho_T t}{WL} \tag{1}$$

where R and ρ represents the resistance and resistivity of the GDL, respectively. Subscripts I and T refer to in-plane and through-plane, respectively; t is the thickness of the GDL, and W and L correspond to the in-plane dimensions of the metal foam pore in contact with the GDL. The ratio of the in-plane to through-plane resistances can be expressed as

$$\frac{R_I}{R_T} \approx \frac{\rho_I}{\rho_T}\frac{L^2}{t^2} \tag{2}$$

The maximum in-plane distance traversed by the electron before it reaches the nearest rib is the pore-size of the metal foam, so $L \approx$ pore size. Since, we are using the same MEA in all of our experiments the thickness of the GDL = 0.3 mm. The in-plane and through-plane resistivity is reported as 0.0065 and 0.071 Ω cm, respectively [16]. Using these values, the ratio in Eq. (2) is calculated to be 6, 1.5 and 0.4 for 10, 20 and 40 ppi metal foams, respectively. Eq. (1) indicates that the effective current collection capability improves monotonically with ppi. However, the detachment and transport of bubbles which influences the effective mass transfer to the catalyst sites decreases with ppi. While this decrease is monotonic, it may be *non-linear* due to the complicated interplay of surface tension, wettability, flow-induced shear, bubble breakup, and so on. Therefore, the combined effect of current collection and bubble removal could present a complex and non-monotonic variation of performance with ppi in the range investigated here (10–40 ppi). However, the explanation provided is qualitative. It would be difficult to estimate each phenomenon quantitatively.

3.2. Effect of foam density on cell performance

The trend in performance with increasing densities of 6–8, 12–16, and 18–24% at a constant pore size of 20 ppi is shown in Fig. 6. Higher density foams possess a smaller pore size in the through-plane direction, but the same in-plane pore size, thus preserving a constant contact area between the metal foam and the carbon cloth. As a result, the current collecting capability

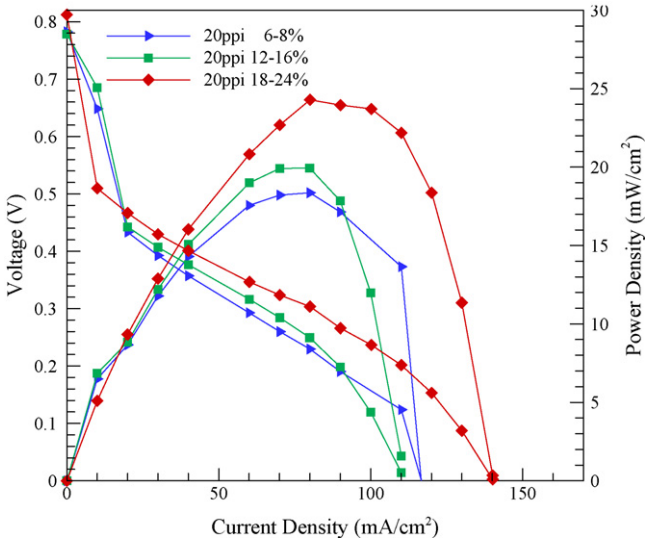

Fig. 6. Comparison of polarization and power density data for DMFC with three different metal foam flow fields (constant ppi but varying density).

is same for all the three foams. However, an increase in foam density reduces its permeability in the in-plane direction and subsequently more methanol would be transported convectively into the underlying GDL making it more available for the reaction at the catalyst sites. Similarly, an increase in foam density also promotes CO_2 removal from the underlying GDL and catalyst layer and helps to open expose new catalyst sites for the reaction. Therefore, higher convective transport with increasing density improves the cell performance. Varying the density at a constant ppi would also affect the gas management characteristics of the metal foam. It should be noted that the flow rate of methanol through metal foams in this set of experiments is too small to cause a noticeable effect on crossover.

CO_2 bubble growth, detachment, and transport are influenced by the through-plane and in-plane metal foam pore characteristics. The metal foam structure will not significantly impede the transport of small bubbles. However, at high current densities, large quantities of carbon dioxide are produced forming large gas slugs whose movement could be impeded by the metal structure. This interference would be greater in 20 ppi, 18–24% density metal foam than 20 ppi, 6–8% density metal foams. The combination of these different effects would influence the polarization curve in a complex manner at high current densities.

3.3. Influence of flow rate and concentration on cell performance

Experiments were conducted to examine the effect of flow rate and concentration (Figs. 7–10) on cell performance with metal foam as the flow field. Fig. 7 indicates that the performance improved moderately with flow rate for the range of flow rates employed. Typically, at a given cell voltage, current density increases as one increases the anode flow rate up to a certain saturation point, beyond which the anode flow rate has no noticeable effect [14]. Therefore, we conclude that the flow rates employed in our experiments were below the saturation

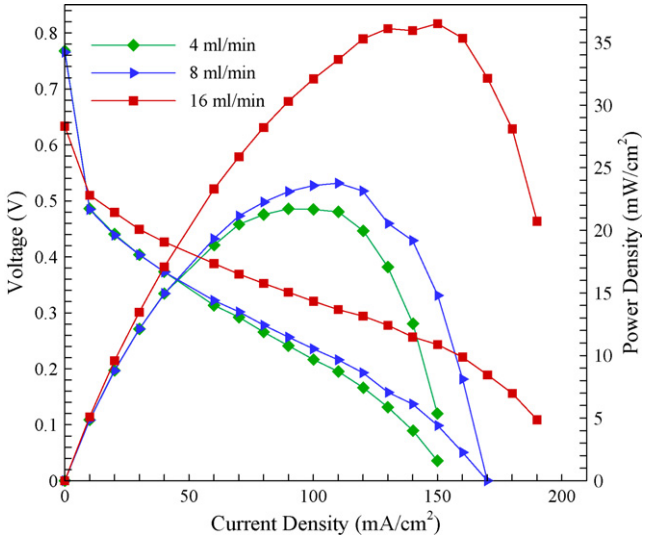

Fig. 7. Comparison of polarization and power density data for DMFC with 40 ppi, 6–8% metal foam flow field for 2 M methanol and three different flow rates.

point. While the polarization curves in Fig. 7 indicate that, the performance improves with flow rate, at the same time the OCV is reduced due to increased crossover.

The velocity of methanol in the GDL can be estimated using Darcy's law, which is based on the theory of flow through porous media; therefore, for the foam as the flow field, the velocity in the underlying GDL is

$$U_G = U_F \frac{K_G}{K_F} \tag{3}$$

here U refers to the velocity of methanol, and K refers to the permeability of the medium. Subscripts G and F refer to the GDL and foam, respectively. We estimate $U_F \approx 0.03\,\mathrm{cm\,s^{-1}}$ at a flow rate of $4\,\mathrm{ml\,min^{-1}}$, with, $K_G \approx 3 \times 10^{-12}\,\mathrm{m^2}$ [16], and $K_F \approx 3 \times 10^{-8}\,\mathrm{m^2}$ [15]. Thus, the velocity of the methanol in the underlying GDL can be calculated using Eq. (3) as $3 \times 10^{-6}\,\mathrm{cm\,s^{-1}}$. Taking the diffusivity of methanol in water as $3 \times 10^{-5}\,\mathrm{cm^2\,s^{-1}}$ and the GDL thickness as 0.3 mm, the Peclet number is estimated to be 0.003. Since the Peclet number is much smaller than unity, we conclude that the methanol transport is diffusion-dominated. Why then do we see an improvement in performance with flow rate in Fig. 7? We believe that this is due to the more effective removal of product CO_2 at higher flow rates. We confirmed diffusion dominance by conducting experiments

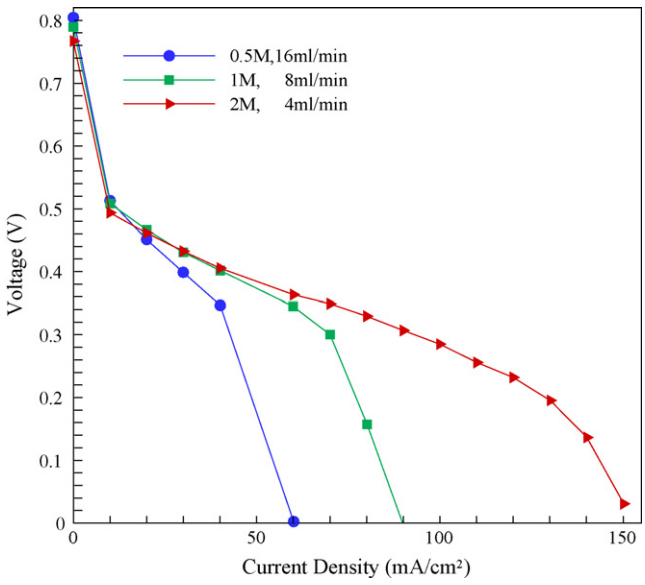

Fig. 8. Comparison of polarization data for DMFC with 40 ppi, 6–8% density metal foam as the flow field with convective mass transport held constant (concentration × flow rate).

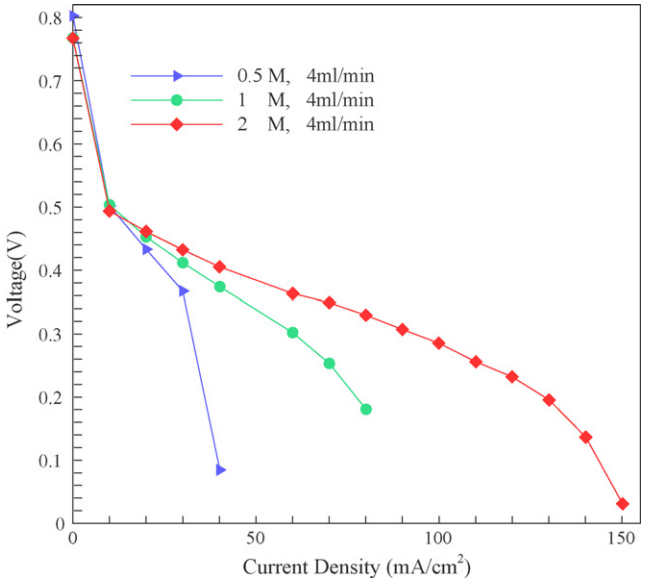

Fig. 9. Comparison of polarization for DMFC with 40 ppi, 6–8% density metal foam flow field for three different concentrations, at a constant flow rate of $4\,\mathrm{ml\,min^{-1}}$.

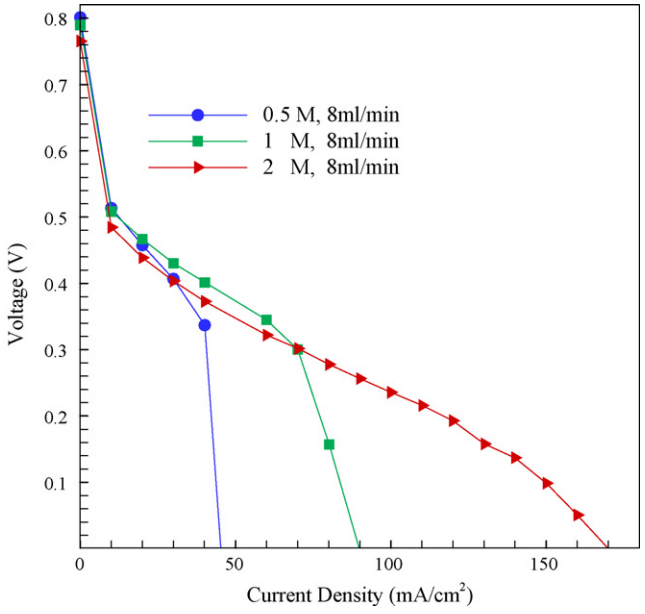

Fig. 10. Comparison of polarization data for DMFC with 40 ppi, 6–8% density metal foam flow field for three different concentrations, at a constant flow rate of $8\,\mathrm{ml\,min^{-1}}$.

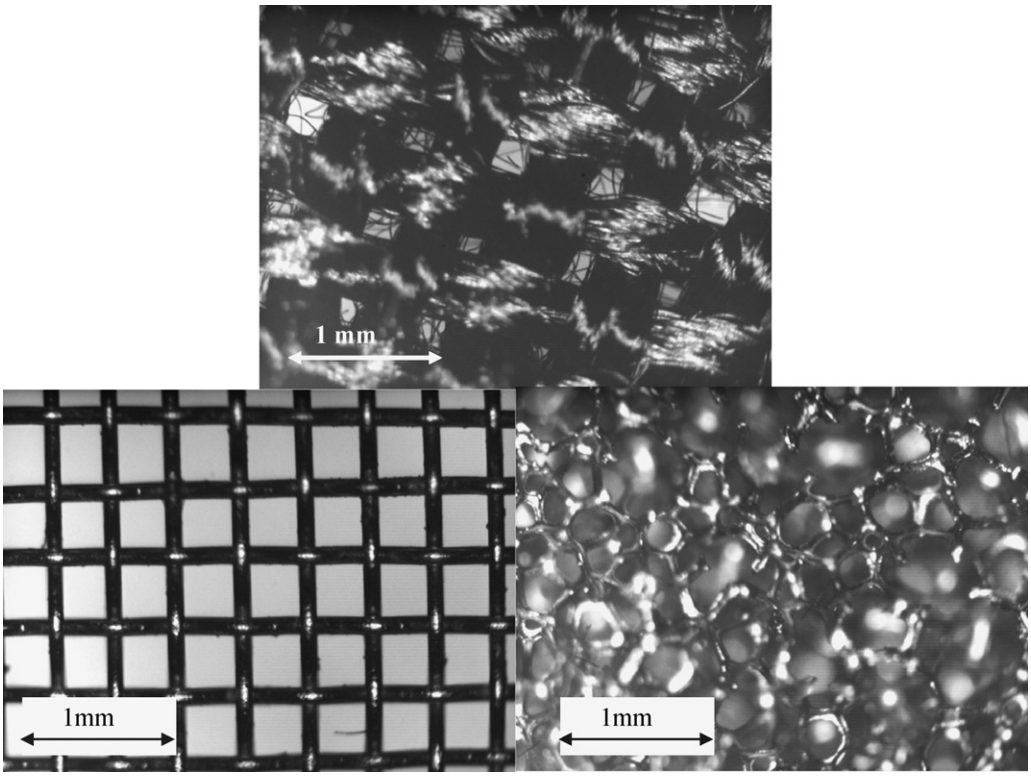

Fig. 11. Microscope images of carbon cloth GDL (top), stainless steel mesh (left), and Ni metal foam (right) after use in the fuel cell.

in which the concentrations and flow rates were simultaneously varied in a manner such that their product remained constant (Fig. 8). We see now that the performance depends strongly on concentration. Furthermore, the effect of increased concentration on performance overwhelms the effect of reduced flow rate.

Figs. 9 and 10 demonstrate the effect of methanol concentration on performance for cells operating at flow rates of 4 and 8 ml min^{-1}, respectively. As expected, higher concentration enhances both the diffusive and convective mass fluxes, and hence a direct dependence on performance is generally observed. However, Fig. 10 indicates that the 1 M, 8 ml min^{-1} cell performs better than the 2 M, 8 ml min^{-1} cell for current densities up to 70 mA cm^{-2}. This can be attributed to the enhanced crossover of methanol at lower current densities. Therefore, an optimal value of concentration and flow rate needs to be chosen for the best performance.

We may conclude from these results that when metal foams are used as the flow field in DMFC, better performance is generally obtained by operating at higher concentrations.

3.4. Polarization behavior and power output with various GDL

Oedegaard et al. [12] reported that carbon cloth performs better than carbon paper for DMFC with a single serpentine flow field. He found that wet proofing (treating with PTFE) accelerates CO_2 transport through the GDL. Wet proofing creates a network of small and large pores in the GDL, allowing CO_2 to escape through the large pores while methanol transports through the small pores [12]. Although adding PTFE reduces the conductivity of the carbon cloth reducing the overall current, greater benefits are realized by minimizing current oscillations due to more stable CO_2 removal.

In the final aspect of this study, we compared cell performance by using a stainless steel metal mesh, and a 94 ppi Ni metal foam as GDL, with a conventional carbon cloth GDL (Fig. 11). The flow field in all three cases was 40 ppi metal foam. Fig. 12 com-

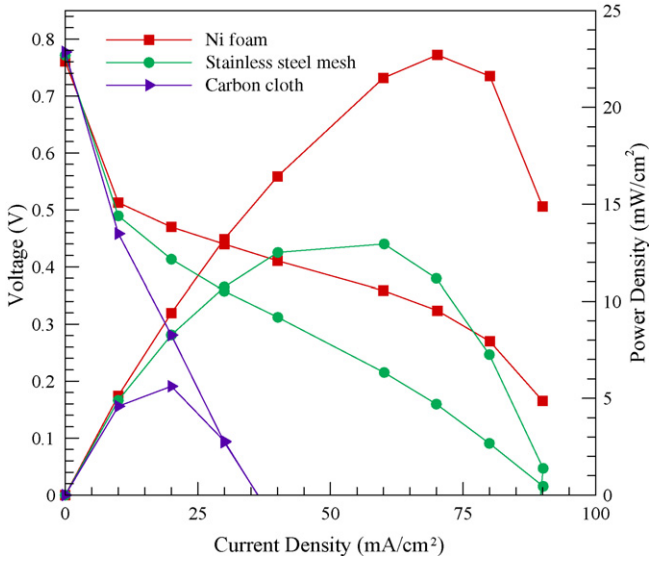

Fig. 12. Comparison of polarization and power density data for DMFC with 40 ppi, 6–8% density foam as the flow field for three different GDLs (i) carbon cloth, (ii) Ni metal mesh, and (iii) Ni metal foam with 94 ppi.

pares the performance of these two novel diffusion layers with carbon cloth. All three MEAs were fabricated in the same way by assembling the diffusion layer against the catalyst-coated membrane. This technique cannot ensure perfect contact between the catalyst-coated membrane and the diffusion layer, and hence resulted in a lower performance.

The stainless steel metal mesh and Ni metal foam show better performance compared to the cloth. The literature indicates that metal mesh as GDL performs better than carbon cloth [12]. The three GDLs were viewed under microscope (Fig. 11) after use in the fuel cell. The pores of the carbon cloth are square with each side measuring ≈0.1–0.25 mm, whereas the pores of the metal foam are circular with average diameter of 0.15 mm. Hence, the larger (on average) pore dimension of the carbon cloth contributes to larger ohmic losses. In addition, upon inspecting the used five-layer MEAs, we found that the membrane had wrinkled, which could trap pockets of CO_2 between the soft carbon cloth GDL and the membrane. On the other hand, the rigid metal foam would suppress the entrapment of pockets of CO_2, which would enhance the contact compared to carbon cloth. The electrical conductivity of Ni is 14 times that of carbon cloth further reducing ohmic losses. Therefore, although the metal foam GDL is thicker than carbon cloth, its increased conductivity and good contact result in higher performance [17]. Since the pore size within the Ni foam is small, contact stresses on the membrane are reduced during cell assembly.

Polarization data were collected by maintaining a constant current density and measuring the corresponding voltage. The MEAs employed for these experiments were fabricated in our laboratory. Hence, they are not treated with PTFE, and therefore a stable current discharge with time is not observed at high current densities. However, comparatively we observed that the metal mesh MEA provided the most stable current discharge, whereas the carbon cloth MEA provided the least stable current discharge. PTFE treatment on metal foams would expectedly enhance the stability of current collection. These experiments opens up the possibility of using metal foams as GDLs compared to traditional carbon cloth and paper.

3.5. Scanning Electron Microscopy inspection of the foam

SEM photos of an unused Al foam sample (Fig. 13, bottom two images) and Al foam subjected to fuel cell conditions for approximately 40 h (Fig. 12, top two images) are shown at 1500 (left) and 400 (right) magnification. Significant corrosion is evident in the used foams. Spectrum processing of the used metal foam confirmed the presence of large amounts of aluminum oxide. The potential difference created across the membrane in

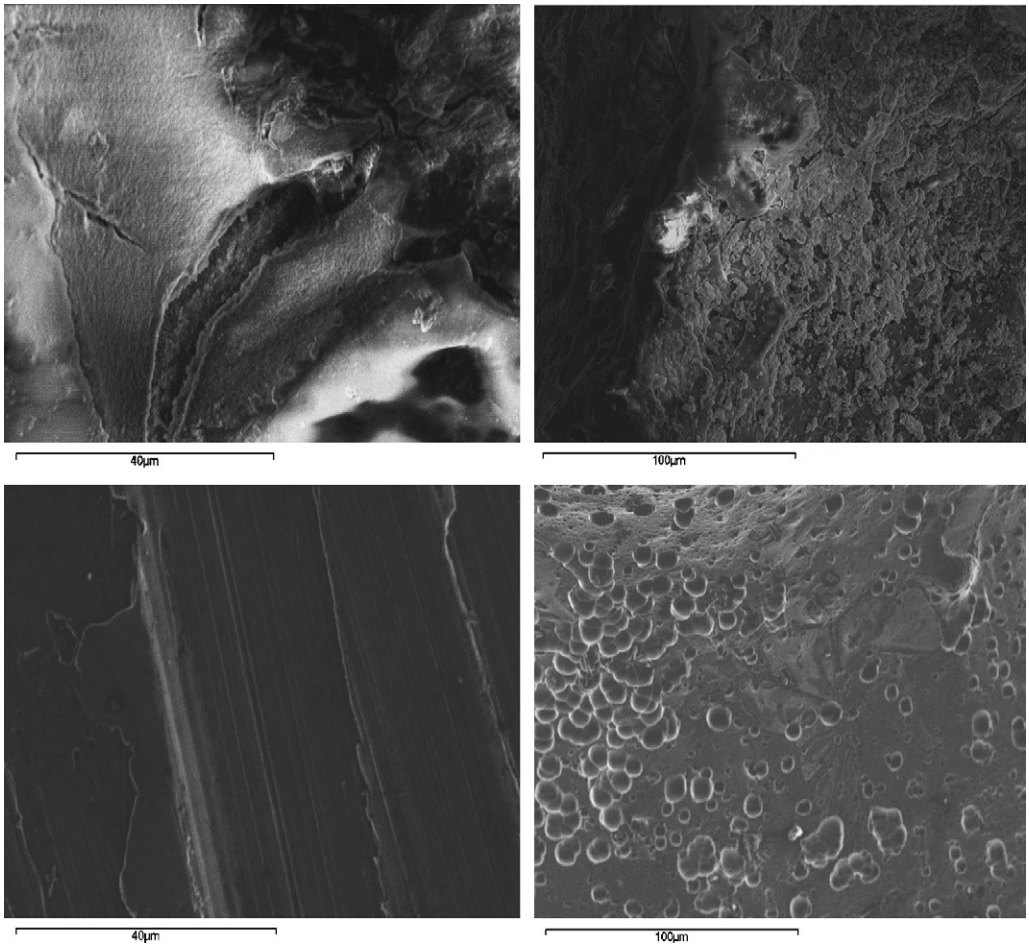

Fig. 13. SEM images of two fresh foam samples (bottom), and two foam samples examined after operating in the fuel cell for a long duration (top).

a working fuel cell also acts across the metal foam, promoting the reaction between the metal foam and methanol, which exacerbates the corrosion process. Ni is more resistant to corrosion compared to aluminum. However, Ni foams are more expensive and less conductive compared to Al foams. Therefore, Ni-coated aluminum foams would be an appropriate choice for such applications.

4. Concluding remarks

Performance studies were conducted with direct methanol fuel cells incorporating metal foams as the flow field and also as GDL. The performance of the metal foam depends on the foam pore size and density. The opposite trends in current collection capability and gas management characteristics cause performance to behave in a complex manner with varying pore size. However, increasing the density at a constant pore size promotes methanol transport and CO_2 removal in the GDL producing a direct improvement in performance. We observed an increase in performance with increasing methanol flow rate and concentration. The strong dependence of performance on methanol concentration is expected because the transport of methanol within the GDL underlying the metal foam is diffusion dominated.

The feasibility of using metal foams as a GDL is also explored. It was found that the metal foams perform better as GDLs compared to cloth and metal mesh. Ni foam has good electrical conductivity compared to that of carbon cloth in which enhances performance. A possible drawback of using metal foam flow fields is their susceptibility to corrosion. This issue must be addressed before they can be effectively used as multifunctional composite materials for structural and power requirements.

Acknowledgements

The authors acknowledge the support of the Delaware Department of Natural Resources and Environmental Control, and Army Research Laboratory.

References

[1] V. Gogel, T. Frey, Z. Yongsheng, K.A. Friedrich, L. Jorissen, J. Garche, J. Power Sources 127 (2004) 172–180.
[2] J.T. South, R.H. Carter, J.F. Snyder, C.D. Hilton, D.J. O'Brien, E.D. Wetzel, Material Research Society Symposium Proceedings vol. 851, Materials Research Society.
[3] A. Kumar, R.G. Reddy, J. Power Sources 129 (2004) 62–67.
[4] A.S. Arico, P. Creti, V. Baglio, E. Modica, V. Antonucci, J. Power Sources 91 (2000) 202–209.
[5] K. Scott, P. Argyropoulos, P. Yiannopoulos, W.M. Taama, J. Appl. Electrochem. 31 (2001) 823–832.
[6] H. Yang, T.S. Zhao, Electrochim. Acta 50 (2005) 3243–3252.
[7] P. Argyropoulos, K. Scott, W.M. Taama, Electrochim. Acta 44 (1999) 3575–3584.
[8] A. Kumar, R.G. Reddy, J. Power Sources 114 (2003) 54–62.
[9] J. Wind, R. Spah, W. Kaiser, G. Bohm, J. Power Sources 105 (2002) 256–260.
[10] D.P. Davies, P.L. Adcock, M. Turpin, S.J. Rowen, J. Appl. Electrochem. 30 (2000) 101–105.
[11] R.C. Makkus, A.H.H. Janseen, F.A. de Bruijn, R.K.A.M. Mallant, J. Power Sources 86 (2000) 274–282.
[12] A. Oedeggard, C. Helbling, A. Schmitz, S.M. Holst, R. Tunold, J. Power Sources 127 (2004) 187–196.
[13] P. Argyropoulos, K. Scott, W.M. Taama, J. Appl. Electrochem. 29 (1999) 661–669.
[14] J. Ge, H. Liu, J. Power Sources 142 (2005) 56–69.
[15] K.C. Leong, L.W. Jin, Int. J. Heat Mass Transfer 49 (2006) 671–681.
[16] M. Mathias, J. Roth, J. Fleming, W. Lehnert, Handbook of Fuel Cells, 2000 (Chapter 46).
[17] C. Xu, T.S. Zhao, Q. Ye, Electrochim. Acta 51 (2006) 5524–5531.